

# Stellar populations in the dwarf spheroidal galaxy Leo I

Filippina Caputo<sup>1</sup>, Santi Cassisi<sup>2</sup>, Marco Castellani<sup>3</sup>, Gianni Marconi<sup>3</sup>

and

Patrizia Santolamazza<sup>1</sup>

## ABSTRACT

We present a detailed study of the color magnitude diagram (CMD) of the dwarf spheroidal galaxy Leo I, based on archival *Hubble Space Telescope* data. Our photometric analysis, confirming previous results on the brighter portion of the CMD, allow us to obtain an accurate sampling of the stellar populations also at the faint magnitudes corresponding to the Main Sequence. By adopting a homogeneous and consistent theoretical scenario for both hydrogen and central helium-burning evolutionary phases, the various features observed in the CMD are interpreted and reliable estimations for both the distance modulus and the age(s) for the main stellar components of Leo I are derived. More in details, from the upper luminosity of the Red Giant Branch and the lower luminosity of the Subgiant Branch we simultaneously constrain the galaxy distance and the age of the oldest stellar population in Leo I. In this way we obtain a distance modulus  $(m - M)_V = 22.00 \pm 0.15$  mag and an age of 10–15 Gyr or 9–13 Gyr, adopting a metallicity  $Z = 0.0001$  and  $0.0004$ , respectively. The reliability of this distance modulus has been tested by comparing the observed distribution of the Leo I anomalous Cepheids in the period-magnitude diagram with the predicted boundaries of the instability strip, as given by convective pulsating models. The detailed investigation of the age (s) of the Leo I stellar populations is then performed by comparing the CMD with a suitable set of theoretical isochrones and central helium-burning models. By taking into account all the various features, including the lack of RR Lyrae variables, we conclude that the star formation process in Leo I has started at  $\sim 10$  Gyr (with  $Z = 0.0001$ ) or  $\sim$

---

<sup>1</sup>Osservatorio Astronomico di Capodimonte, Via Moiariello 16, 80131 Napoli, Italy; caputo@astrna.na.astro.it, patrizia@cerere.na.astro.it

<sup>2</sup>Osservatorio Astronomico di Collurania, Via Maggini, 64100 Teramo, Italy; cassisi@astrte.te.astro.it

<sup>3</sup>Osservatorio Astronomico di Roma, Via Frascati 33, 00040 Monteporzio; mkast@coma.mporzio.astro.it, marconi@coma.mporzio.astro.it

13 Gyr (with  $Z=0.0004$ ) ago and it stopped about 1 Gyr ago. Some evidence is reported supporting the mild metal deficiency ( $Z=0.0004$ ), whereas no clear indication has been found supporting a star formation history characterized by episodic bursts. The adoption of updated physics which includes the inward diffusion of elements, as recently presented for globular cluster stars, would yield a slightly larger distance modulus ( $\sim 0.10$  mag) and a slightly lower age for the most ancient stellar component ( $\sim 1$  Gyr).

*Subject headings:* galaxies: dwarf, galaxies: individual (Leo I), stars: distances, stars: horizontal branch, stars: variables: general

## 1. Introduction

Many of the nine dwarf spheroidal galaxies (dSphs) clustering around the Milky Way are known to have had a complicated evolutionary history as suggested from clear evidences of star formation, continuously or in bursts, over a wide period of time (see, e.g., Mighell 1997 [Carina], Beauchamp et al. 1995 [Fornax], Lee et al. 1993 [Leo I], Mighell & Rich 1996 [Leo II], Da Costa 1984 [Sculptor], and the comprehensive review by Mateo 1998).

For the not-too-far dSphs, several CMDs that reached the main-sequence turnoff (MSTO) have been published, allowing the analysis of their stellar content. For the more distant galaxies, only in the very recent time the *Hubble Space Telescope* is providing the deep CMDs (see, e. g., Mighell & Rich 1996) that are necessary to fully understand the evolutionary history of these faint members of the Local Group (van den Bergh 1994).

In this work we present a study of the stellar populations in the dSph Leo I, based on archival Wide Field Planetary Camera 2 (WFPC2) data. This galaxy, discovered by Harrington & Wilson (1950) during the first Palomar sky survey, is thought to be among the most distant satellites of the Milky Way and therefore it plays an important role in determining the mass of our galaxy (Zaritsky et al. 1989; Zaritsky 1991). On the other hand, the variable star survey carried out by Hodge & Wright (1978) showed an unusual large number of anomalous Cepheids, and the CMD published by Lee et al. (1993 [L93]) "...shows no suggestion for any Horizontal Branch typical of other dSphs". Furthermore, it should be added that all the published CMDs (see also Fox & Pritchett 1987; Reid & Mould 1991; Demers, Irwin & Gambu 1994 [DIG]) *suggest* that the stars of Leo I have a younger mean age than that of the other dSphs, but the so far published data - even those from the deepest CCD photometry - do not reach the faint magnitudes we need to estimate definitively the stellar age(s).

Section 2 deals with the observations and data reduction. The CMD for Leo I is discussed in Section 3, together with a review of former works on this galaxy. The theoretical scenario used for interpreting the stellar content of Leo I is presented in Section 4, while our original analysis, with a discussion of the resultant distance and age, is given in Section 5. The summary of the main results follows in Section 6.

## 2. Observations and data reduction

The data for Leo I have been requested and retrieved electronically from the ESO/ST-ECF archive in Garching (Munich). The galaxy was observed with the *Hubble Space Telescope* WFPC2 on 1994 March 5 through the F555W ( $\sim V$ ) and F814W ( $\sim I$ ) filters.

The WFPC2 aperture was centered on the target position  $\alpha_{2000} = 10^h 08^m 26.58^s$ ,  $\delta_{2000} = 12^\circ 18' 33.4''$ , and eight observations were obtained: three 1900 s plus one 350 s exposures in F555W, and three 1600 s plus one 300 s exposures in F814W. These observations (part of the HST Cycle 4 program GTO/WFC 5350) were placed in the public data archive on 1995 March 5.

Correction to the raw data for bias, dark and flat-field were performed using the standard HST pipeline. Subsequent data reduction, for the WF cameras, was made using MIDAS routines ROMAFOT and DAOPHOT II packages. The next steps were schematically as follows. First, a filter median was applied upon each frame, using a software in ROMAFOT in order to remove cosmic rays from single frames.

To push the star detection limit to as faint a level as possible, we coadded all images taken through the same filter. Then, we used the deepest I coadded frame to search for stellar objects in each chip. All the objects identified in this search were fitted in all frames I and V using DAOPHOT II and the hybrid weighted technique described by Cool and King (1995). Two DAOPHOT detection passes were carried out, separated by photometry and subtraction of all stars found in the first pass. Faint stars hidden within the PSF skirts of brighter companions were thereby revealed and added to the list of detected stars to be measured. For each chip and each filter the PSF was build by using not less than 15 bright and isolated stars in each frame. The single measures were averaged, and an average instrumental magnitude was derived for each object in each colour.

A total of 36.634 stars were ultimately detected and measured in the three WFs frames. Corrections to 0.5'' aperture were made in each case; we transformed the F814W and F555W instrumental magnitudes into the WFPC2 "ground system" using Eq. 6 of Holtzman et al. (1995).

Completeness tests were carried out by adding 5% of the original number of stars for each selected bin (0.4 mag) of magnitudes to the original coadded F555W and F814W frames. 'Artificial' stars were added randomly with the same instrumental color distribution of the real stars detected in the frames. The 'artificial' frames were then processed using DAOPHOT II in a manner identical to that applied to the original data. The completeness was finally derived as the ratio  $N_{rec}/N_{add}$  of the artificial stars generated. We have considered as recovered only those stars which have been found in the same spatial position and inside the same magnitude bin with respect to the added stars. The results of these tests are shown in Table 1, which shows that the 50% completeness level occurs at F555W  $\sim 26.0$ . Since we only perform qualitative analysis, i.e., we do not make comparisons between observative/theoretical luminosity functions, such a procedure is fully satisfactory for the present investigation.

The internal errors were also estimated computing the rms frame to frame scatter of the instrumental magnitudes obtained for each stars (see Table 2).

Recently, the Leo I galaxy has been also studied by Gallart et al. (1999). They choose to normalize their HST photometry to L93 calibration. According to the quoted authors, the L93 photometry is regarded as reliable, because the large number of calibration stars in their field. With the aim to check qualitatively our photometry, we made the colours distribution histogram of the objects belonging to the clump of stars near the Red Giant Branch with magnitude in the range  $21.5 \leq V \leq 22.6$  mag (see Fig. 1 and the following discussion); a comparison with the same histogram realized by L93 (see their Figure 8) shows that the peaks of the two distributions fall in the same color bin (i.e.,  $0.80 \leq (V - I) \leq 0.85$ ). Such result make us quite confident on the reliability of our photometry: differences between our calibration and that of L93 are inside the adopted bin width (i.e.,  $\Delta(V - I) = 0.05$ ). For a detailed star-by-star comparison, we address the interested reader to Gallart et al. (1999).

### 3. CMD of Leo I

As already stated, this section deals with the main features of the CMD of Leo I stars as well as with a review of previous works. In our belief, this would provide the best framework for our results, presented in the following sections.

#### 3.1. General morphology

The  $V$ - $(V - I)$  color-magnitude diagram of Leo I, as based on 36.634 stars down to a limiting magnitude of  $V \sim 27.5$  mag ( $I \sim 26.5$  mag) is displayed in Fig. 1. The principal features, which are discussed in detail in the following section, are here summarized.

*Red Giant Branch.* There is a well-defined red giant branch (RGB) with the tip (TRGB) seen at  $V_{TRGB} \sim 19.4 \pm 0.10$  mag ( $I_{TRGB} \sim 18.0 \pm 0.10$  mag), in agreement with the L93 study. The few stars located above the TRGB are likely to belong to the asymptotic giant branch (see L93 and DIG). The observed color dispersion read at  $V=20.0$  mag ( $\simeq 0.5$  mag below TRGB) is  $\Delta(V - I) \sim 0.10$  mag, which is slightly larger than the L93 value (0.08 mag). It is known that the color dispersion along RGB can derive from photometric errors as well as from metallicity and age spread. However, at  $V=20.0$  mag the mean photometric error (see Table 2) is  $\sim 0.015$  mag, leaving an intrinsic dispersion of  $(0.10^2 - 0.015^2)^{0.5} = 0.098$  mag which will be discussed in the following.

*Horizontal Branch.* As already shown from previous studies, there is no evidence of the "flat" portion of the horizontal branch (HB) which is typical of Galactic globular clusters and other dSphs. However, the clump of red giant stars seen at  $(V - I) \sim 0.7-0.9$  mag and  $21.5 \leq V \leq 22.6$  mag are *bona fide* central helium-burning stars, even though more massive than those observed in old stellar systems. The sequence of stars with  $20.0 \leq V \leq 21.5$  and  $0 \leq (V - I) \leq 0.7$  could represent the more massive tail of these helium-burning stars (see Section 4).

*Main Sequence stars.* The most impressive feature in the color-magnitude diagram of Leo I is the MSTO region seen at  $V \sim 22.60 \pm 0.20$  mag, which is also the luminosity of the faintest helium-burning clumping stars (the lower envelope of HB stars is taken at  $V_{HBLE} = 22.60 \pm 0.05$ ). Such a feature would suggest by itself the presence of stars with age near 1–2 Gyr (see Caputo & Degl'Innocenti 1995). Moreover, there is also a small group of brighter main-sequence stars with  $21.0 \leq V \leq 22.6$  mag. These "blue stragglers" could be mass transfer binaries or, if normal main sequence stars, they might be witnesses of a small population of very young stars. Beside the above clear evidence of a young stellar component, one notices the well developed subgiant branch extending below the clumping red giant stars. The faint stars at the base of the subgiant branch (BSGB) are seen at  $(V - I) \sim 0.8$  mag and  $V_{BSGB} = 25.00 \pm 0.20$  mag. The observed difference in magnitude between the TRGB and BSGB stars is  $\Delta V(BSGB - TRGB) \sim 5.6$  mag, which is similar to the values observed in the CMDs of Galactic globular clusters, thus suggesting an old stellar population of  $\sim 10-15$  Gyr.

### 3.2. Variable stars

As stated at the very beginning, the most striking difference between Leo I and the other dwarf spheroidals is the lack of RR Lyrae stars and, conversely, the large number of anomalous Cepheids. Hodge & Wright (1978) measured blue magnitude, period and amplitude for 12 variables (with an estimate of 75% completeness), while L93 suggested that the 45 stars observed with  $21.2 \leq V \leq 19$  mag and  $0 \leq (V - I) \leq 0.6$  mag are anomalous Cepheid candidates. None of the Hodge & Wright (1978) variables are located in our color-magnitude diagram and for the stars in our CMD seen with  $20.0 \leq V \leq 21.5$  and  $0 \leq (V - I) \leq 0.6$  we have no way to confirm the variability.

### 3.3. Metallicity and reddening

There are somewhat conflicting results concerning the mean metallicity of Leo I. Previous estimates based on CMD features vary from  $[\text{Fe}/\text{H}] = -1.0 \pm 0.3$  (Reid & Mould 1991), to  $[\text{Fe}/\text{H}] = -1.6 \pm 0.4$  [DIG] and  $[\text{Fe}/\text{H}] = -2.1 \pm 0.1$  [L93], depending on the assumed distance modulus, while moderate resolution spectra of two red giants (Suntzeff 1992, see L93) suggest  $[\text{Fe}/\text{H}] \sim -1.8$ . On the other hand, we show in Section 4 that the occurrence of a significant number of anomalous Cepheids is by itself a clear indication that Leo I is a metal-poor stellar system with an overall metallicity between  $Z = 0.0001$  and  $0.0004$  (see also Castellani & Degl’Innocenti 1995; Caputo & Degl’Innocenti 1995; Bono et al. 1997 [BCSCP]).

As for the reddening, the relatively high galactic latitude of Leo I suggest a low foreground reddening. The blue extinction reported by Burstein & Heiles (1984) is  $A_B = 0.09$  mag. On this basis, following the Cardelli, Clayton & Mathis (1989) relations, we will adopt  $E(B - V) = 0.02$  mag and  $E(V - I) = 0.04$  mag.

### 3.4. Distance and Age

Given the lack of HB stars at the RR Lyrae gap, previous estimates of the Leo I distance have mostly used the TRGB [L93:  $(m - M)_0 = 22.18 \pm 0.11$  mag], the median magnitude of the red giant clump [DIG:  $(m - M)_0 = 21.7 \pm 0.12$  mag] and the carbon stars [DIG:  $(m - M)_0 = 21.5 \pm 0.3$  mag]. As early discussed by DIG, the problem with these distance indicators is that the results depend on the adopted metallicity (see also Cassisi, Castellani & Straniero 1994) in the sense that the deduced distance modulus increases with decreasing the metal content. We wish to add that some of the theoretical constraints discussed in this paper suggest a dependence of the TRGB luminosity on the age which has to be taken into account when dealing with young stellar populations.

As for the age, the absence of blue horizontal branch, the presence of several carbon stars, and the clumping red giant stars yielded DIG to suggest an upper age limit of  $\sim 7$  Gyr for the dominant stellar population, with no obvious evidence of an older stellar component (their CMD does not reach the main sequence turnoff). The deeper CCD photometry presented by L93 revealed an increased number of main sequence stars at  $V \sim 23.5$  mag, consistent with the presence of young stars of  $\sim 3$  Gyr. More recently, the L93 measurements have been interpreted by Caputo, Castellani & Degl’Innocenti (1995, 1996) as evidence of even younger stellar populations ( $\sim 2.0$ – $1.5$  Gyr).

#### 4. Theoretical background

In order to provide a clear and complete reference framework, let us summarize the primary theoretical constraints which are relevant for the present investigation. They are derived from the evolutionary models (both hydrogen and central helium-burning phases) with masses from  $0.6M_{\odot}$  to  $2.2M_{\odot}$ , original helium  $Y_0=0.23$  and metallicity  $Z=0.0001$ ,  $0.0004$  already presented by Castellani & Degl’Innocenti (1995) and BCSCP.

As a first point, we show in Fig. 2 theoretical isochrones with  $Z=0.0001$  and selected ages, transformed into the observational plane  $M_V-(V-I)$  by means of the stellar atmosphere models provided by Castelli, Gratton & Kurucz (1997a,b). Besides the well known evidence that with increasing age the RGB color becomes redder and the MSTO point becomes fainter, one notices the clear variation of the TRGB luminosity, which fades at the lower ages. As shown in the lower panel of Fig. 3, where the predicted absolute magnitude of TRGB is plotted versus the age, such a behaviour is less pronounced with  $Z=0.0004$ . For the purpose of present paper, we present in the upper panel of Fig. 3 the corresponding variation of the luminosity at the base of the subgiant branch.

From the theoretical isochrones with  $Z=0.0001$  we derive that at  $M_V=-2.0$  mag ( $\sim 0.5$  mag below TRGB) the color variation with age is

$$(V-I)_{M_V=-2} = 1.13 + 0.11 \log t, \quad (1)$$

while the  $Z=0.0004$  isochrones are redder by  $\Delta(V-I) \sim 0.04$  mag, at constant age. Such a result yields that the predicted contribution of the age to the observed color dispersion along RGB is significantly larger than previously adopted. As an example, L93 assumes a difference  $\Delta(V-I)=0.03$  mag between the 3.5 and 15 Gyr isochrones, whereas the present results would give  $\sim 0.07$  mag. On these grounds, one understands that it is necessary to estimate the actual age spread before deriving the metallicity dispersion from the observed RGB width.

Passing to the central helium-burning phase, let us remind that for stellar structures experiencing a strong He-flash, i.e. for evolving masses smaller than  $\approx 1.0M_{\odot}$ , the age  $t_{fl}$  and the mass  $M_{c,fl}$  of the He-core at the RGB tip depend slightly on the evolutionary mass, but significantly on the chemical composition. On the contrary, when increasing the stellar mass, these evolutionary parameters strongly depend on both the mass (as a consequence of the changes in the electron degeneracy level inside the core during the RGB evolution) and chemical composition. The data listed in Table 3 and plotted in Fig. 4 show that, if the mass  $M_{pr}$  of the star is lower than  $\approx 2.2M_{\odot}$ , then both  $t_{fl}$  and  $M_{c,fl}$  are decreasing functions of  $M_{pr}$ . The consequences on the subsequent zero age horizontal branch (ZAHB) are easily understandable (see also Castellani & Degl’Innocenti 1995; Caputo & Degl’Innocenti 1995).

With increasing the age, the maximum permitted mass  $M_{HB,max}$  for central He-burning stars ( $M_{HB,max}$  is equal to the mass of the RGB progenitor  $M_{pr}$  in the hypothesis of no mass-loss during the RGB phase) decreases, whereas, following the corresponding variation of  $M_{c,fl}$ , the luminosity of the ZAHB model at  $(V - I)_0 \sim 0.70$  mag tends to increase (see last column in Table 3).

On the other hand, the evolutionary calculations show that the effective temperature of a ZAHB model decreases with increasing the mass, reaching the minimum value of  $\log T_e \sim 3.74$  ( $Z=0.0001$ ) or  $\sim 3.72$  ( $Z=0.0004$ ) around  $1.0-1.2 M_\odot$ . After that, the more massive models with  $Z=0.0001$  present higher luminosity and larger effective temperature, causing a ZAHB "turn-over" and the development of a "upper horizontal branch" (UHB). On the contrary, the models with  $Z=0.0004$  and mass in the range of  $1.3M_\odot$  to  $1.5M_\odot$  are characterized by higher luminosity and roughly constant effective temperature. Consequently, with  $Z=0.0004$  the ZAHB "turnover" is occurring after  $1.5M_\odot$ .

All these features are presented in Figures 5 and 6, where ZAHB sequences (solid line) of stars with the same RGB progenitor (see the labelled  $M_{pr}$ ) but having experienced different degrees of mass-loss, are displayed. The same figures show the post-ZAHB evolution of the most massive ( $M_{HB,max}=M_{pr}$ ) central He-burning model (dashed line). Note that a further increase of the metallicity up to  $Z=0.001$  would shift the ZAHB "turn-over" to masses significantly larger than  $2.0M_\odot$  (Demarque & Hirshfeld 1975; Hirshfeld 1980).

In order to have an immediate insight into the connection between the central-helium burning evolution and radial pulsation, we show in Figures 7a and 7b the evolution of HB models with mass  $M_{HB}=M_{pr}$ , but with the effective temperature of the model scaled to the red edge of the instability strip (FRE). The location of FRE, as well as the adopted width of the instability strip, is provided from the pulsational models discussed by BCSCP.

The first straightforward result is that He-burning stars with evolutionary mass in the range of  $\sim 1.0M_\odot$  to  $\sim 1.2M_\odot$  (for  $Z=0.0001$ ) or in the range of  $\sim 0.8M_\odot$  to  $\sim 1.7M_\odot$  (for  $Z=0.0004$ ) are confined near the red giant branch, out of the instability strip. Thus, no variable stars are expected within these mass ranges. Moreover, one derives that the lowest mass for the occurrence of massive pulsators brighter than RR Lyrae stars, i.e. anomalous Cepheids, is  $1.3M_\odot$  with  $Z=0.0001$  and  $1.8M_\odot$  with  $Z=0.0004$ . In terms of age, this could mean that the anomalous Cepheids should have ages younger than  $\sim 3$  and  $1$  Gyr, with  $Z=0.0001$  and  $Z=0.0004$ , respectively (see Table 3). Finally, one may notice that with  $t_{fl} \sim 15$  Gyr the evolution of the most massive HB model at  $Z=0.0004$  ( $M_{HB} = M_{pr} = 0.75M_\odot$ ) is confined at the red side of the RR Lyrae instability strip, whereas with  $Z=0.0001$  the most massive HB model ( $0.80M_\odot$ ) evolve within the instability strip. Thus, *even with a null mass-loss*, central He-burning stars with  $Z=0.0001$  and age  $\sim 15$  Gyr are expected to

populate the RR Lyrae gap.

### 5. Revising the distance modulus and the age of Leo I

The theoretical isochrones presented in Fig. 2 show that with increasing age the maximum luminosity of RGB stars increases whereas the minimum luminosity of SGB stars decreases. Thus, if composite stellar populations are present in Leo I, then the oldest stars have to be seen at BSGB and TRGB. By starting from these simple considerations, we combine in Fig. 8 the theoretical data already shown in Fig. 3 with the observed values  $V_{TRGB} = 19.40 \pm 0.10$  mag and  $V_{BSGB} = 25.00 \pm 0.20$  mag, aiming at checking the possibility of a unique solution for the Leo I distance modulus by using these two observables. As a result, we obtain that the apparent distance modulus of Leo I, as given from its oldest stellar component, is  $(m - M)_V = 22.00 \pm 0.15$  mag. Moreover, the data in Fig. 8 suggest that the age of these stars is in the range of 10.0–15.0 Gyr and 9.0–13.0 Gyr, with  $Z=0.0001$  and  $Z=0.0004$ , respectively. However, if further observations will confirm the lack of RR Lyrae stars, then from the data plotted in Fig. 7a we could add that the Leo I oldest stellar component cannot be older than  $\sim 10$  Gyr, with  $Z=0.0001$ .

We can straightway check the derived distance modulus  $(m - M)_V = 22.00 \pm 0.15$  mag by comparing observed data of Leo I anomalous Cepheids with the theoretical predictions given by the BCSCP pulsating convective models. Figure 9 shows the period–luminosity diagram for Leo I variables<sup>4</sup>. It is quite evident that the predictions conform very well to the observed data, supporting the above distance modulus.

The comparison between theoretical isochrones and the CMD of the stars in Leo I, corrected with  $(m - M)_V = 22.00$  mag and  $E(V - I) = 0.04$  mag, is displayed in Fig. 10a ( $Z=0.0001$ ) and Fig. 10b ( $Z=0.0004$ ). As a whole, these figures provide further support to the result that the oldest stars in Leo I were formed  $\sim 10$  Gyr or  $\sim 13$  Gyr (with  $Z=0.0001$  and  $0.0004$ , respectively) ago. Moreover, the brightest MSTO stars seen at  $V \sim 22.60 \pm 0.20$  mag conform quite well the 1 Gyr isochrones, while the bright blue stragglers should have even younger ages ( $\sim 700$  Myr). The absence of distinct MSTOs, as those seen in Carina (see Smecker–Hane et al. 1996), gives evidence against episodic bursts and, as a whole, we conclude that Leo I has forming stars rather continuously, even though at lower level during the last billion years, from about 10 Gyr or 13 Gyr ago (depending on the adopted metallicity) to at least  $\sim 1$  Gyr ago. Our conclusions are not discordant with the results

---

<sup>4</sup>The  $B$ -magnitudes from Hodge & Wright (1978) are corrected with  $(m - M)_B = 22.02$ , according to the adopted reddening  $E(B - V) = 0.02$  mag.

of Gallart et al. (1998) which suggest that Leo I experienced a major increase of star formation from  $\sim 6$  to 2 Gyr ago, with some prior episodes lasting 2-3 Gyr and a decreasing activity until 500-200 Myr ago.

The derived spread of ages leads [see Eq. (1)] to a predicted color dispersion along RGB of  $\sim 0.11$  mag, which is consistent with the intrinsic RGB width ( $\sim 0.10$  mag). This result seems to exclude a substantial metallicity dispersion of the Leo I stars. On the other hand, it has been shown that the presence of anomalous Cepheids is a clear indication of young ( $\leq 3$  Gyr) *and* metal-poor ( $Z \leq 0.0004$ ) stellar population. Thus, we are able to conclude that the actual metal dispersion content of Leo I is at the most in the range of  $Z=0.0001$  to  $Z=0.0004$ .

It has been shown (see, e.g., Caputo & Degl’Innocenti 1995) that in stellar systems in which is present a *not-too-old* stellar population, the observed star distribution along the RG clump can provide safe constraints on the allowed range of stellar ages. Now we wish to adopt a similar approach to investigate how the above age dispersion agrees with the observed clump of central helium-burning stars. For this aim, the CMD of Leo I stars with  $V \leq 23.00$  mag is displayed in Fig. 11 together with HB evolutionary tracks with  $Z=0.0001$  and  $M_{HB} = M_{pr}$  (the dashed line refers to the model with  $2.0M_{\odot}$ ), and by adopting the two extreme values of the distance modulus derived from the previous analysis. With  $(m - M)_V=21.85$  mag (lower panel), the absolute magnitude of the lower envelope is equal to  $M_V^{HBLE}=0.75\pm 0.05$  mag, suggesting (see Table 3) that the stars at the HBLE are  $\sim 2$  Gyr old and have a RGB progenitor with mass  $M_{pr} \sim 1.4M_{\odot}$ . However, when considering the mass distribution along the corresponding ZAHB locus, the mass of the star at  $(V - I)_0 = 0.7$  mag is of about  $0.8M_{\odot}$ , a result which would imply a substantial mass-loss during the RGB phase (or at the He-flash).

As for the remaining stars forming the clump seen at  $(V - I) \sim 0.7-0.9$  mag and  $21.5 \leq V \leq 22.6$  mag, the comparison with our HB evolutionary models shows that they are matched by the HB evolution of models with mass ( $M_{HB} = M_{pr}$ ) equal to  $0.9M_{\odot}$  ( $\sim 10$  Gyr),  $1.0M_{\odot}$  ( $\sim 7$  Gyr) and  $1.2M_{\odot}$  ( $\sim 4$  Gyr). Similarly, the stars with  $20.0 \leq V \leq 21.5$  and  $0 \leq (V - I) \leq 0.7$ , which observationally define the UHB, appear reasonably fitted with more massive (and younger) HB models from  $1.4M_{\odot}$  (2.2 Gyr) up to  $\sim 2.0M_{\odot}$  ( $\sim 0.7$  Gyr), assuming no mass-loss. Let us notice, that we are not neglecting the possibility that a mass-loss phenomenon could affect the progenitors of such HB structures during the RGB evolution. Here we are interested only to the location in the CMD of the more massive (and brightest) HB star for each fixed assumption on the RGB progenitor. All the other less massive ZAHB structures are located at lower luminosity (see previous discussions and Caputo & Degl’Innocenti 1995). For the same reason, in principle it could be possible

that such CMD region is populated by HB structures with still more massive - and then younger - RGB progenitor, which have suffered an efficient mass-loss phenomenon during the previous evolutionary phase. Nevertheless, this occurrence does not seem supported at all by the comparison between the full CMD diagram and theoretical isochrones, performed in Fig. 10.

By adopting  $(m - M)_V = 22.15$  mag (upper panel), the absolute magnitude of the HBLE stars  $M_V^{HBLE} = 0.45 \pm 0.05$  mag, which is consistent with the location of the 10 Gyr old ZAHB (corresponding to the  $0.9M_\odot$  progenitor) and masses (on the ZAHB) near  $0.9M_\odot$ , thus implying a negligible mass-loss. As a whole, for the clumping red giant stars with  $(V - I) \sim 0.7-0.9$  mag and  $21.5 \leq V \leq 22.6$  mag we derive masses (during the central He-burning phase) from  $0.9$  to  $1.3M_\odot$  and ages in the range of 10 to 3 Gyr, respectively, assuming no mass-loss for the RGB progenitor. As for the UHB stars with  $20.0 \leq V \leq 21.5$  and  $0 \leq (V - I) \leq 0.7$ , they appear somehow brighter than the evolutionary tracks of the most massive (and younger) models, rather supporting the smaller distance modulus. In passing, we wish to note the fine agreement between the shape of the observed clump of stars and the location of our HB tracks. However, we notice also some discrepancy between observed data and theoretical models with  $Z=0.0001$  as due to the blue loop of the evolutionary sequences which extends hotter than the observed color of the clumping stars.

As shown in Fig. 12, such a discrepancy is removed if the  $Z=0.0004$  models are taken into consideration. By adopting  $(m - M)_V = 21.85$  mag (lower panel), the HBLE stars turn out to be  $\sim 2.3$  Gyr old, with a mass near  $0.75M_\odot$  to be compared with  $M_{pr} = 1.4M_\odot$ . On the other hand, the remaining clumping red giants with  $(V - I) \sim 0.7-0.9$  mag and  $21.5 \leq V \leq 22.6$  mag agree with the HB evolution of models from  $0.80$  to  $1.4M_\odot$  and ages from 13 to 2.3 Gyr, respectively, assuming no mass-loss. Similarly, the brightest stars with  $20.0 \leq V \leq 21.5$  and  $0 \leq (V - I) \leq 0.7$  seem to require masses up to  $2.2M_\odot$  (dotted line), assuming no mass-loss for the progenitor. Adopting  $(m - M)_V = 22.15$  mag (upper panel) yields that the absolute magnitude of the HBLE stars is somehow brighter than the  $0.80M_\odot$  model with age of  $\sim 13$  Gyr (i.e. the maximum age derived from isochrone fitting), suggesting that the distance modulus of Leo I is not larger than  $(m - M)_V = 22.00$  mag. With such a value, we derive that the HBLE stars have mass  $0.80M_\odot$  and age  $\sim 13$  Gyr, while for the remaining clumping red giant stars we obtain  $1.0-1.6M_\odot$  and 1-7 Gyr, respectively, assuming no mass-loss. However, also for this metallicity the fit of the UHB stars seems to support the smaller distance modulus.

In conclusion, by taking into account all the various features of the CMD, our best estimates for the metallicity and the distance modulus of Leo I are  $Z=0.0004$  and  $(m - M) = 21.90 \pm 0.05$  mag. The resulting ages of the stellar components are from 1 to 13

Gyr, with few stars as young as  $\sim 700$  Myr, as derived from theoretical isochrones and HB evolutionary models. Finally the analysis of the clumping red giants seem to suggest that the younger stellar populations (i.e. those with massive RGB progenitors) suffered a substantial mass-loss during the RGB phase or at the He-flash.

Before closing this analysis, it seems worth mentioning that the recent improvements of the stellar evolutionary models have produced younger ages for the Galactic globular clusters (see, e.g., Cassisi et al. 1998 and references therein). Even though the whole "improved physics" is subject of deep investigation (Castellani & Degl'Innocenti 1998), we decided to compute a set of "new" evolutionary models with  $Z=0.0002$ , taking into account also the inward diffusion of helium and heavy elements. From the new isochrones shown in figure 13, we obtain slightly larger distance modulus ( $(m - M)_V=22.10 \pm 0.15$  mag) and ages in the range of  $\sim 0.7$  to 10 Gyr. As for the He-burning stars, the new models yield that the red giant clumping stars have ages and masses in the range of  $\sim 1$  to 10 Gyr and  $0.85$  to  $1.3M_\odot$  respectively, while the UHB stars require masses up to  $2.2 M_\odot$  (see figure 14).

## 6. Summary

As clearly stated in several works (see the comprehensive review by Mateo (1998) and reference therein) the possibility to obtain a deep insight into the intrinsic evolutionary properties of the main stellar population(s) in dSphs represents a pivotal tool in order to understand not only the properties of our nearest extragalactic neighbours but also to improve our knowledge of the Galaxy. Indeed, the decoding of the evolution history of dSphs in the Local Group sheds light on the formation and evolution of our own Milky Way. Moreover, a thorough understanding of the evolution history of dSphs and more in general of the Local Group is a fundamental precondition in order to understand the observational features of high-redshift, unresolvable galaxies. However, it is clear that accurate analysis of the star formation history and reliable knowledge of age(s) and metallicity distribution rely on several observational features, as derived from as much accurate as possible CMD diagrams reaching the faintest Main Sequence magnitudes. In the present analysis we have adopted this approach in order to investigate into the stellar populations of the dSph galaxy Leo I. The more relevant points can be summarized as it follows.

- By using HST archival data, an accurate photometric investigation has been carried out. This occurrence has allowed us to obtain a CMD with more than 36.600 stars which reaches very faint magnitudes ( $V \sim 27.5$  mag). The tests performed during the photometric analysis show that our photometry reaches the 50% completeness level at the magnitude (F555W)  $\approx 26.0$ .

- The CMD of Leo I is characterized by a well-defined RGB and by a HB clumped near the RGB. The observed TRGB is seen at  $V=19.40\pm 0.10$  mag and the HB morphology does not show any evidence for a *flat* distribution near the RR Lyrae instability strip. Moreover, the well developed SGB extends below the red giant clump, down to  $V=25.00\pm 0.20$  mag and the brightest MSTO is located at  $V \sim 22.60 \pm 0.20$  mag, with some few stars even brighter and bluer.
- By adopting a reference theoretical scenario for both hydrogen and central helium-burning stars with  $Z=0.0001$  and  $Z=0.0004$ , the observed maximum luminosity of RGB and minimum luminosity of SGB are used to derive a distance modulus of  $(m - M)_V=22.00\pm 0.15$  mag. Furthermore, the resulting estimates for the age of the oldest stellar population turn out to be in the range of 10–15 Gyr and 9–13 Gyr with  $Z=0.0001$  and 0.0004, respectively. However, when considering also the lack of RR Lyrae stars in Leo I, we conclude that the oldest stellar component in Leo I is at the most 10 Gyr old, with  $Z=0.0001$ .
- Such distance modulus evaluation has found further support by comparing the distribution of anomalous Cepheids in the  $\langle M_B \rangle - \log P$  plane with the location of the instability strip boundaries, as predicted by convective pulsating models.
- By adopting the above distance modulus, the comparison of the Leo I CMD with theoretical isochrones yields that the brightest MSTO stars are consistent with an age of the order of 1 Gyr, for both the two adopted metallicities.
- When all these evidences are accounted for, it is possible to reach the conclusion that the star formation process in Leo I has started at about 10 Gyr or 13 Gyr ago, depending on the adopted metallicity, and it stopped about 1 Gyr ago, without any clear evidence for the star formation occurring by single episodic bursts. This results appear in satisfactory agreement with the scenario outlined by Mateo (1998, his figure 8b) and Grebel (1998);
- such a dispersion of age is consistent with the mass of central helium-burning stars, which are derived to be in the range of  $0.75\text{--}0.9M_\odot$  to  $2.0\text{--}2.2M_\odot$ , depending on the adopted metal content.
- The estimated age range of the main stellar components in Leo I provides a consistent explanation for the observed color spread along RGB, without the need for invoking a substantial metallicity dispersion as early suggested by L93.
- Finally, the use of the theoretical evolutionary scenario based on a updated physical inputs (Cassisi et al. 1998) does not change in remarkable way the results achieved:

the main effects are a slight increase of the distance modulus ( $\sim 0.10$  mag) and a slight decrease of the age for the older stellar component ( $\sim 1$  Gyr).

We are grateful to an anonymous referee for the pertinence of her/his comments regarding the content and the style of an early draft of this paper, which improved its readability.

## REFERENCES

- Aparicio, A., Gallart, C., 1995, AJ, 110, 2105
- Beauchamp, D., Hardy, E., Suntzeff, N. B., & Zinn, R. 1995, AJ, 109, 1628
- Bono, G., Caputo, F., Santolamazza, P., Cassisi, S., & Piersimoni, A. 1997, AJ, 113, 2209 [BCSCP]
- Burstein, D. & Heiles, C. 1984, ApJS, 54, 33
- Caputo, F., & Degl’Innocenti, S. 1995, A&A, 298, 833
- Caputo, F., Castellani, V., & Degl’Innocenti, S. 1995, A&A, 304, 365
- Caputo, F., Castellani, V., & Degl’Innocenti, S. 1996, A&A, 309, 413
- Cardelli, J. A., Clayton, G. C., & Mathis, J. S. 1989, ApJ, 345, 245
- Cassisi, S., Castellani, V., & Straniero, O. 1994, A&A, 282, 353
- Cassisi, S., Castellani, V., Degl’Innocenti, S., & Weiss, A. 1998, A&AS, 129, 267
- Castellani, V., & Degl’Innocenti, S. 1995, A&A, 298, 827
- Castellani, V., & Degl’Innocenti, S. 1998, *in preparation*
- Castelli, F., Gratton, R.G., & Kurucz, R.L. 1997a, A&A, 318, 841
- Castelli, F., Gratton, R.G., & Kurucz, R.L. 1997b, A&A, 324, 432
- Cool, A.M., & King, I.R. 1995, in “Calibrating HST: Post Servicing Mission”, eds. A. Koratkar & C. Leitherer (Baltimore: STScI), p. 290
- Da Costa, G. S. 1984, ApJ, 285, 483
- Demarque, P. & Hirshfeld, A. W. 1975, ApJ, 202, 346
- Demers, S., Irwin, M.J., & Gambu, I. 1994, MNRAS, 266, 7 [DIG]
- Fox, M. F. & Pritchett, C. J. 1987, AJ, 93, 1381
- Gallart, C., Freedman, W., Aparicio, A., Bertelli, G., & Chiosi, C. 1998, AAS Meeting, 192, 7701

- Gallart, C., Freedman, W., Mateo, M. *et al.*, to be published in ApJ, April 1, 1999 (vol.514, n.2), (*astro-ph/9811122*)
- Grebel E. K. 1998, "Star Formation Histories of Local Group Dwarf Galaxies" to be published in the proceedings of the XVIIIth Moriond conference on "Dwarf Galaxies and Cosmology", Les Arcs, March 1998, eds. T. X. Thuan, C. Balkowski, V. Cayatte, J. Tran Thanh Van, Editions Frontieres (*astro-ph/9806191*)
- Harrington, R. G. & Wilson, A. G. 1950, PASP, 62, 118
- Hirshfeld, A. W. 1980, ApJ, 241, 111
- Hodge, P. W. & Wright, F. W. 1978, AJ, 83, 228
- Holtzman, J.A. *et al.* 1995, PASP, 107, 1065
- Lee, M. G., Freedman, W., Mateo, M., Thompson, I., Roth, M., & Ruiz, M.-T. 1993, AJ, 106, 1420 [L93]
- Mateo M. 1998, ARA&A, 36 435 *astro-ph/9810070*
- Mighell, K. J. & Rich, R. M. 1996, AJ, 111, 777
- Mighell, K. J. 1997, AJ, 114, 1458
- Reid, N. & Mould, J. 1991, AJ, 101, 1299
- Smecker-Hane, T.A., Stetson, P.B., Hesser, J.E., & Lehnert, M.D., 1994 AJ, 108, 507
- Van den Bergh, S. 1994, ApJ, 428, 617
- Zaritsky, D., Olszewski, E. W., Schommer, R. A., Peterson, R. C., & Aaronson, M. 1989, ApJ, 345, 759
- Zaritsky, D. F. 1991, Ph.D. Thesis, 19

### Figure captions

Fig. 1.— The  $V$  vs  $(V - I)$  color magnitude diagram of 36.634 stars in Leo I down to a limiting magnitude of  $V \sim 27.5$  mag. The photometric errors at different magnitudes have been also plotted (see Table 2).

Fig. 2.— Theoretical isochrones for  $Y=0.23$ ,  $Z=0.0001$  and ages from 1 to 10 Gyr (left to right).

Fig. 3.— Predicted absolute magnitude at the tip of RGB (lower panel) and at the base of SGB (upper panel) as a function of age and for the two selected metallicities.

Fig. 4.— The behavior of the age  $t_{fl}$  (lower panel) and mass of the He- core  $M_{c,fl}$  (upper panel) at the He ignition as a function of the mass  $M_{pr}$  of the red giant progenitor and for the two selected metallicities.

Fig. 5.— ZAHB sequences (solid line) with  $Z=0.0001$  of stars with the same RGB progenitor (see the labelled masses) and different degree of mass-loss. In each panel, the dashed line refers to the evolution off ZAHB of the HB model with mass  $M_{HB} = M_{pr}$ .

Fig. 6.— As fig. 5, but for  $Z=0.0004$ .

Fig. 7.— *Panel a)*: The H-R diagram for HB models with  $Z=0.0001$  and mass ( $M_{HB} = M_{pr}$ ) as labelled, but with the effective temperature scaled to the red edge of fundamental pulsator strip. The vertical lines define the boundaries of the instability strip. *Panel b)*: as in panel a, but for  $Z=0.0004$ .

Fig. 8.— The distance modulus - age diagram for the oldest stellar component of Leo I, as obtained by using the observational measurements for the TRGB (filled circles) and BSGB (open circles) magnitudes, and the theoretical constraints provided in Figure 3.

Fig. 9.— The period-luminosity diagram for anomalous Cepheids in Leo I in comparison with the predicted limits for pulsation. Solid and dashed lines refer to  $Z=0.0001$  and  $Z=0.0004$ , respectively.

Fig. 10.— *Panel a)*: comparison between the CMD of Leo I and theoretical isochrones for  $Z=0.0001$  and ages from 700 Myr to 15 Gyr. *Panel b)*: as in panel a), but with a metallicity  $Z=0.0004$  and ages in the range from 1 to 15 Gyr.

Fig. 11.— CMD of stars with  $V \leq 23.00$  mag in comparison with HB models with  $Z=0.0001$  and mass  $M_{HB} = M_{pr}=0.9, 1.0, 1.2, 1.4, 1.6, 1.8M_{\odot}$  (solid line) and  $2.0M_{\odot}$  (dashed line) for two different assumptions on the Leo I distance modulus.

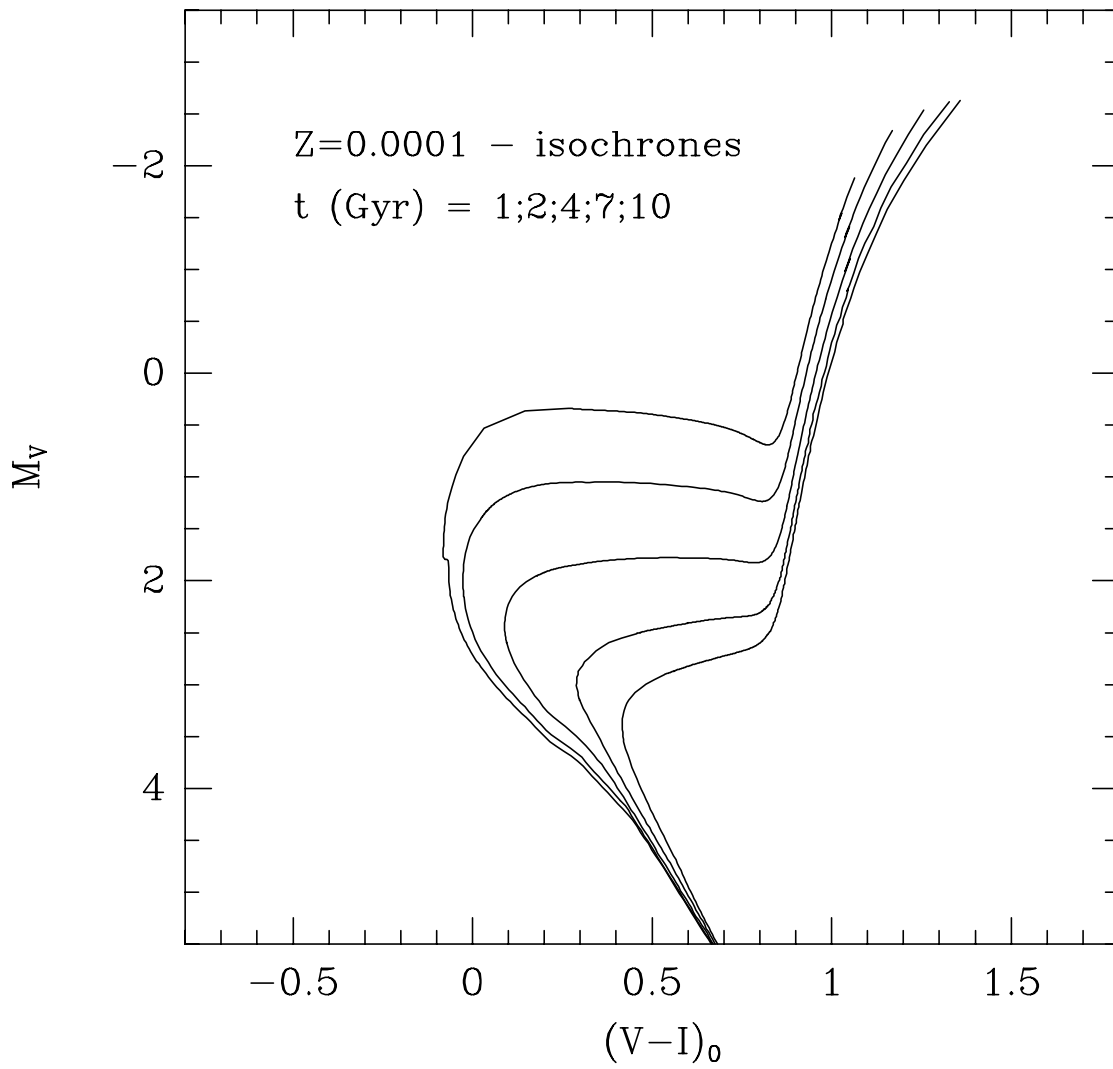
Fig. 12.— As in Fig. 11, but for HB models with  $Z=0.0004$  and mass  $M_{HB} = M_{pr}=0.75, 1.0, 1.2, 1.4, 1.6, 1.8M_{\odot}$  (solid line),  $2.0M_{\odot}$  (dashed line) and  $2.2M_{\odot}$  (dotted line).

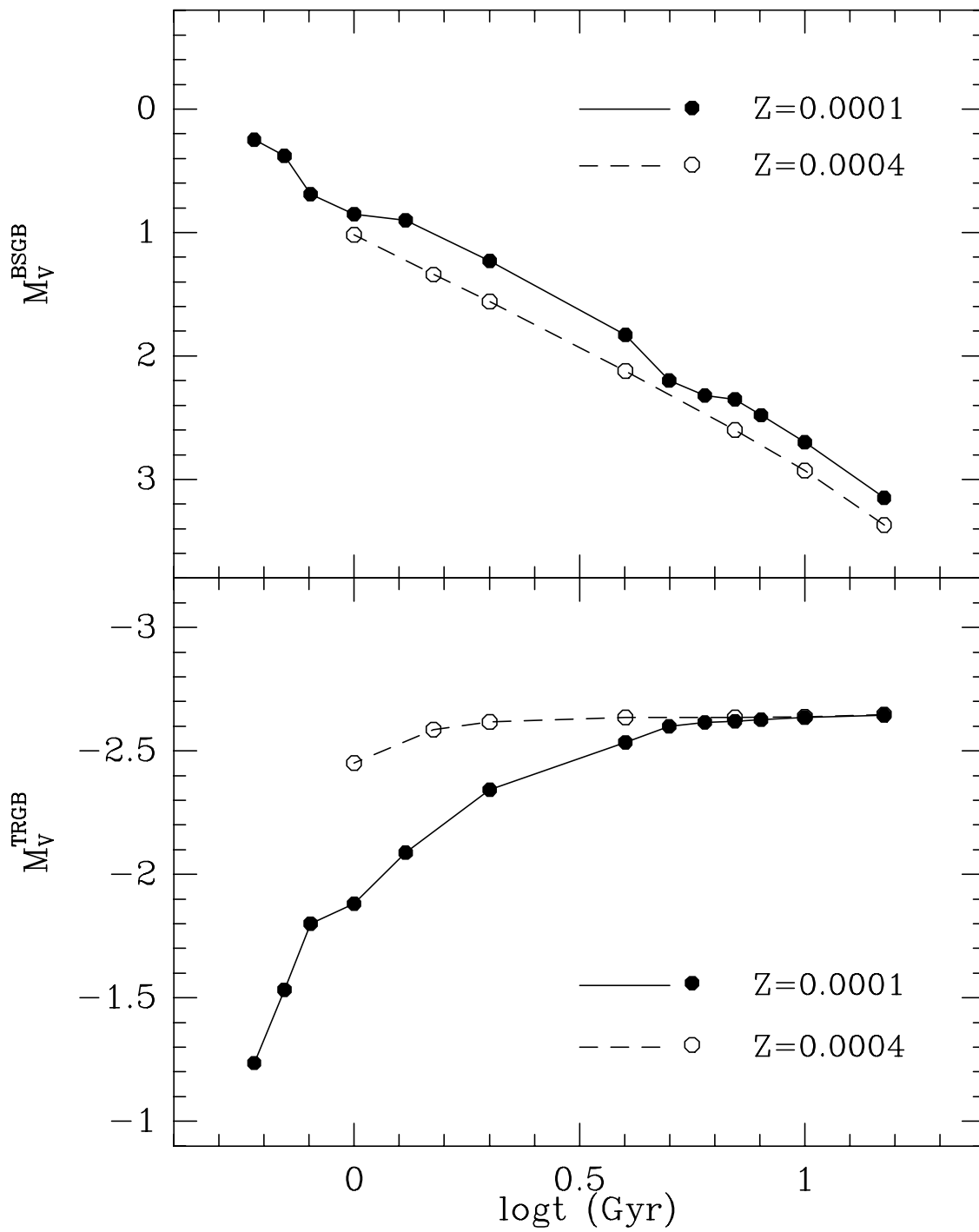
Fig. 13.— Comparison between the CMD of Leo I with a selected set of isochrones, computed by adopting updated evolutionary models (see text for more details), for  $Z=0.0002$  and for the labelled ages. The adopted values for the distance modulus and the reddening are labelled.

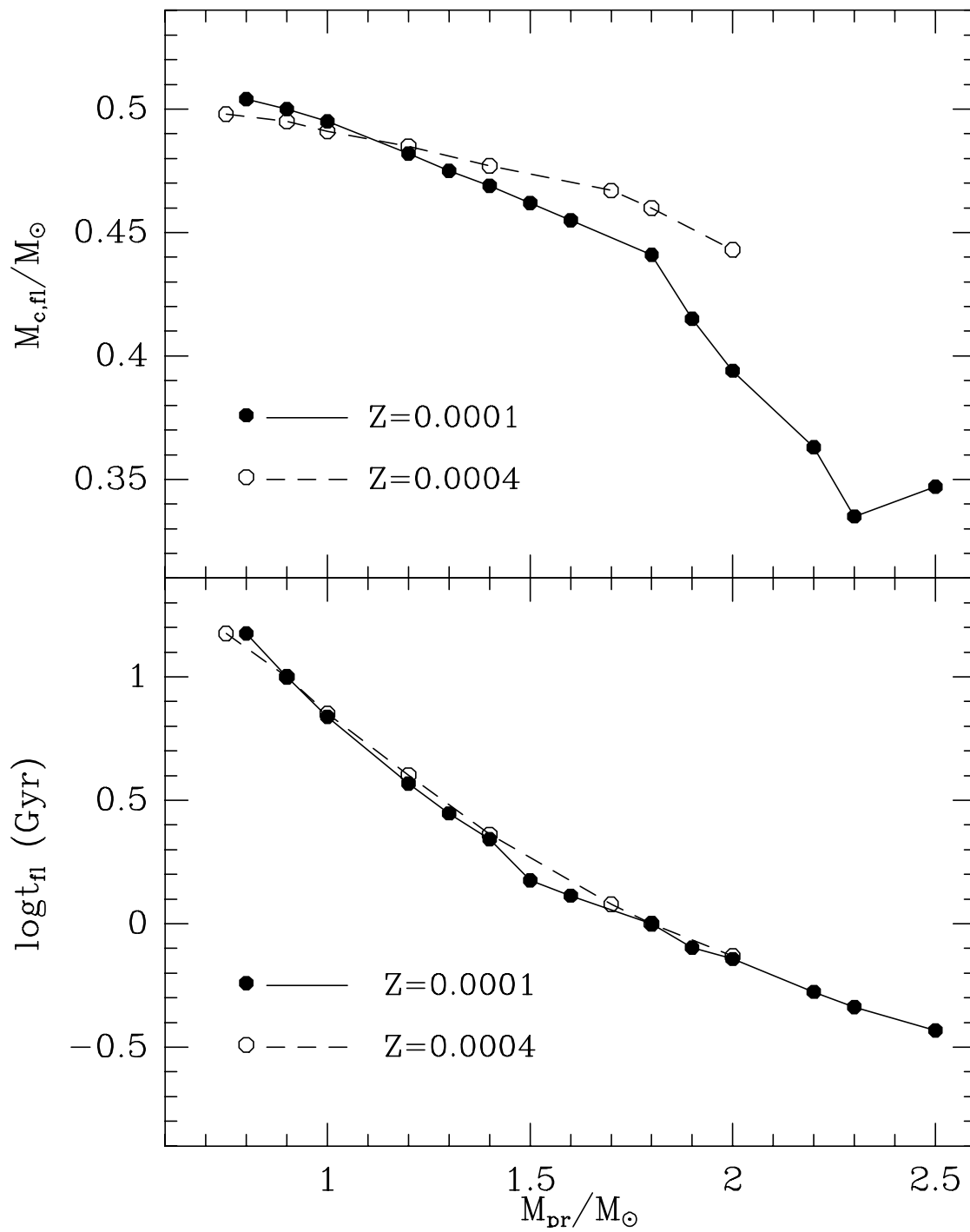
Fig. 14.— Comparison between the CMD diagram location of the HB stars in Leo I and updated evolutionary models (see text) for  $Z=0.0002$ , for two different assumptions on the distance modulus. The stellar masses are  $M_{HB} = M_{pr}=0.85, 1.2, 1.5, 1.8M_{\odot}$  (solid line) and  $2.2M_{\odot}$  (dotted line).

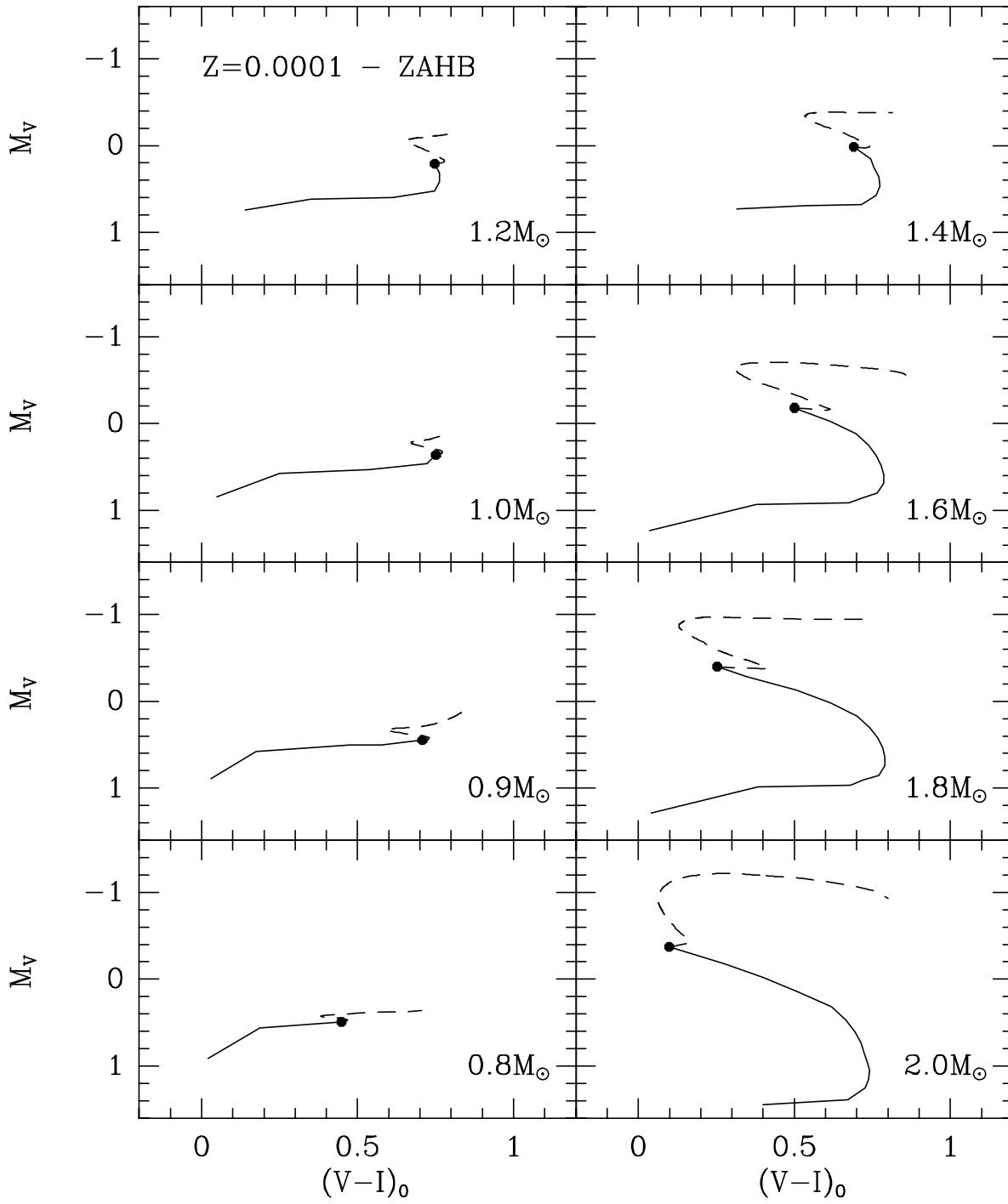
This figure "fig1.gif" is available in "gif" format from:

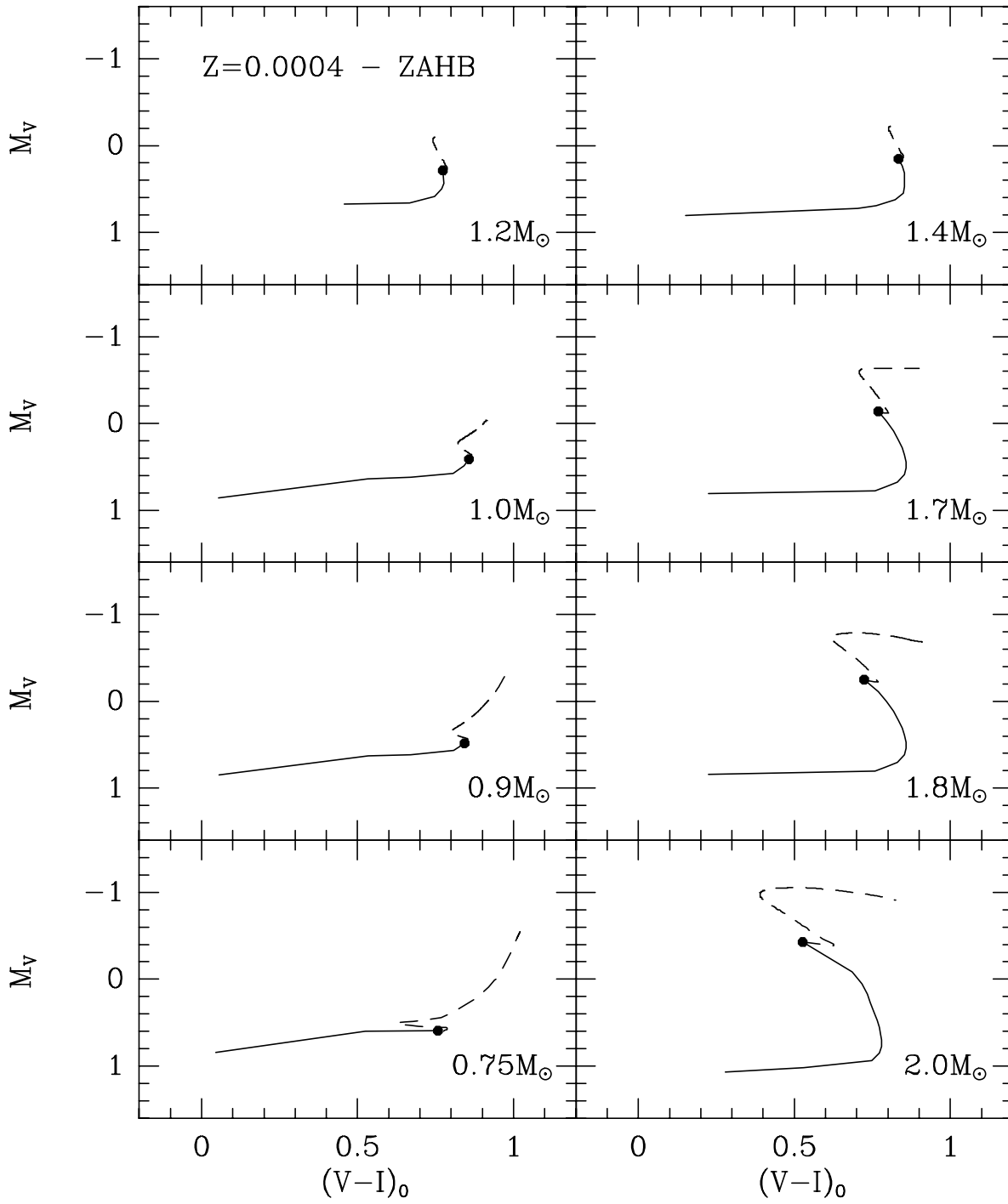
<http://arxiv.org/ps/astro-ph/9812266v1>

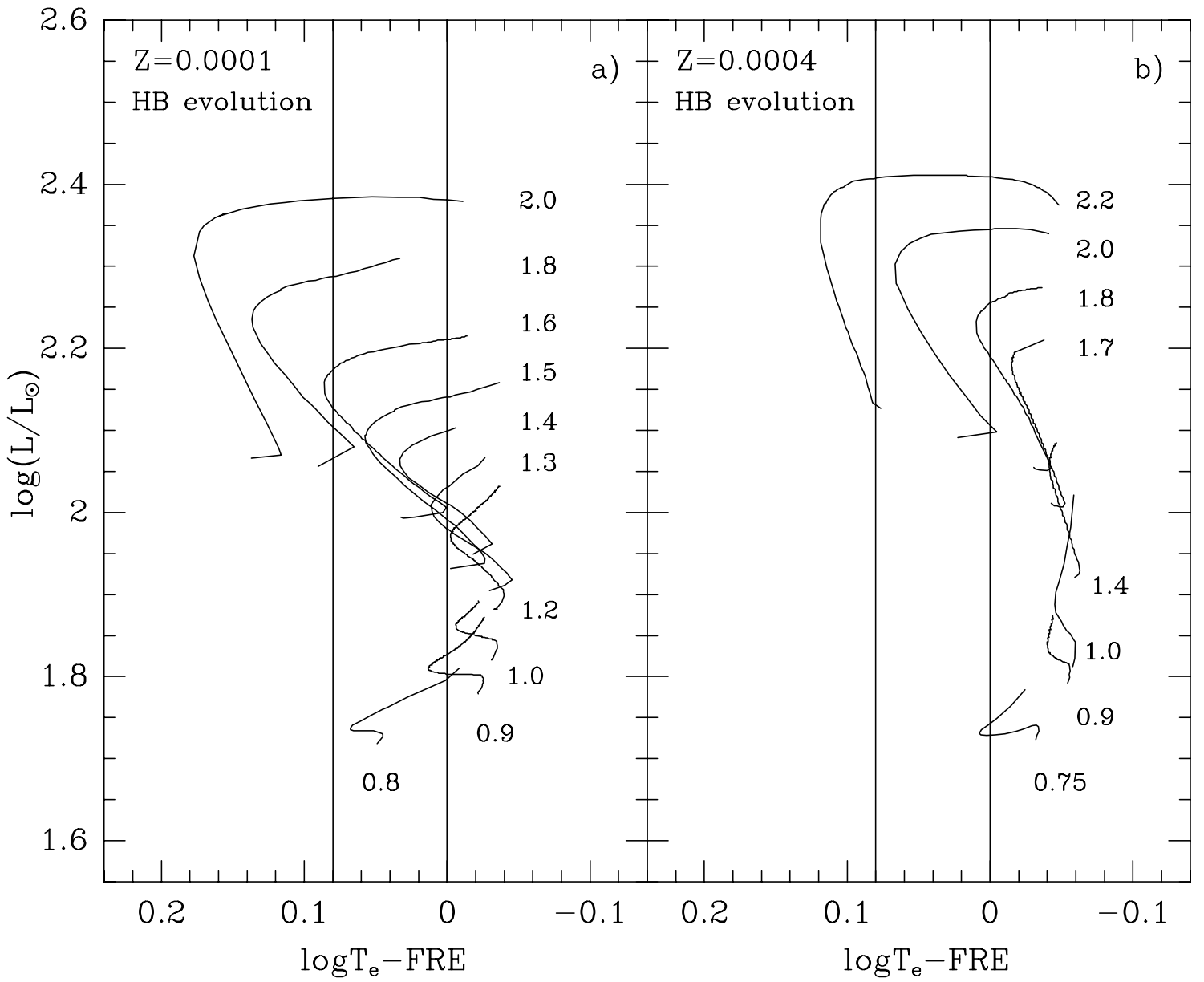


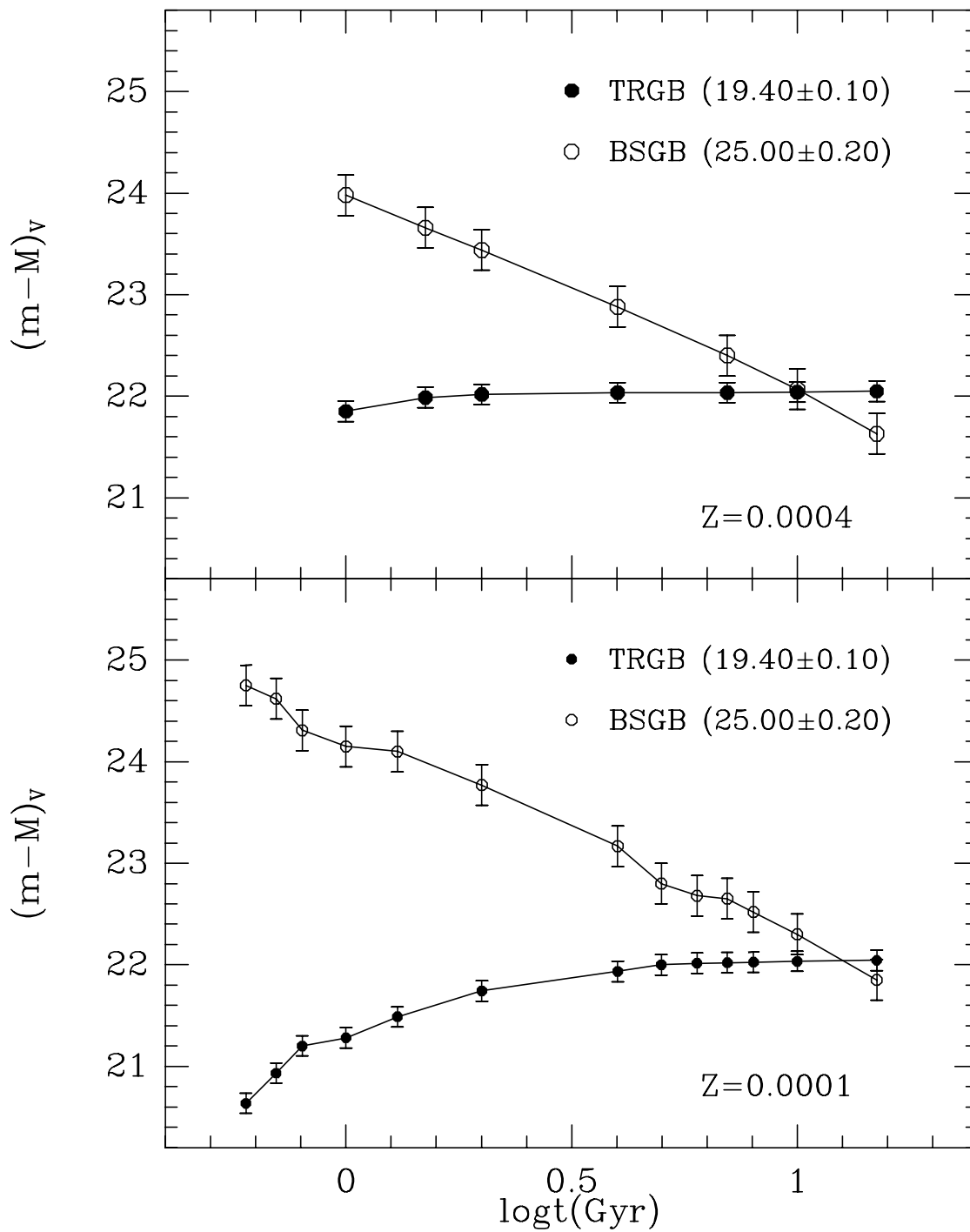


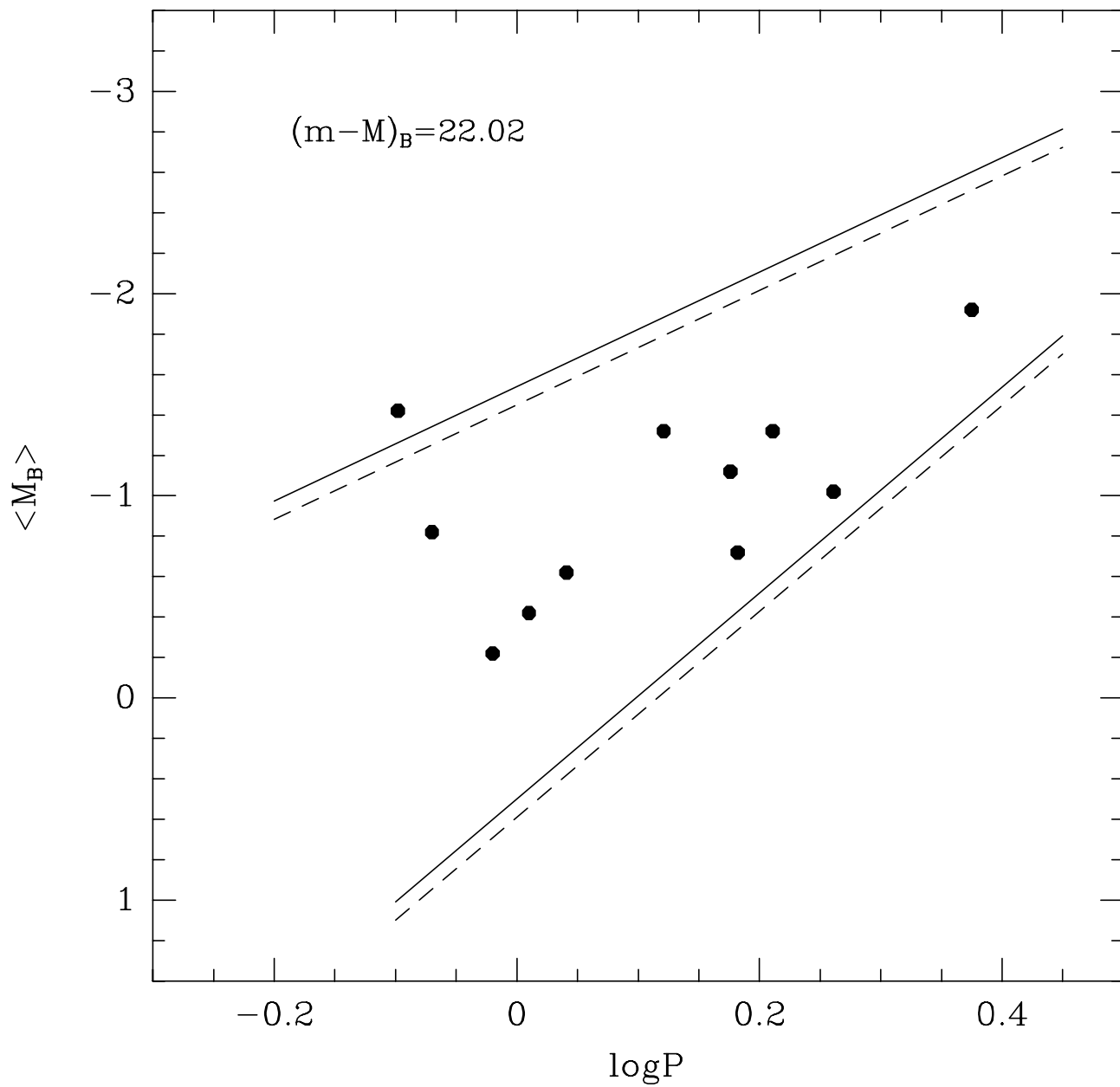












This figure "fig10.gif" is available in "gif" format from:

<http://arxiv.org/ps/astro-ph/9812266v1>

This figure "fig11.gif" is available in "gif" format from:

<http://arxiv.org/ps/astro-ph/9812266v1>

This figure "fig12.gif" is available in "gif" format from:

<http://arxiv.org/ps/astro-ph/9812266v1>

This figure "fig13.gif" is available in "gif" format from:

<http://arxiv.org/ps/astro-ph/9812266v1>

This figure "fig14.gif" is available in "gif" format from:

<http://arxiv.org/ps/astro-ph/9812266v1>

TABLE 1  
RESULTS OF COMPLETENESS TEST.

$\Delta V$	Completeness (%)
25.2-25.6	100
25.6-26.0	76
26.0-26.4	45
26.4-26.8	26
26.8-27.2	8
27.2-27.6	1

TABLE 2  
PHOTOMETRIC ERRORS AT THE CORRESPONDING MAGNITUDE BIN.

$Vbin$	$\Delta V$	$\Delta(V - I)$
18.0-18.5	0.003	0.005
18.5-19.0	0.005	0.008
19.0-19.5	0.007	0.013
19.5-20.0	0.011	0.014
20.0-20.5	0.012	0.015
20.5-21.0	0.015	0.016
21.0-21.5	0.016	0.018
21.5-22.0	0.018	0.022
22.0-22.5	0.020	0.026
22.5-23.0	0.022	0.031
23.0-23.5	0.033	0.043
23.5-24.0	0.040	0.053
24.0-24.5	0.046	0.061
24.5-25.0	0.058	0.083
25.0-25.5	0.069	0.104
25.5-26.0	0.082	0.123
26.0-26.5	0.098	—
26.5-27.0	0.121	—

TABLE 3

SELECTED THEORETICAL EVOLUTIONARY QUANTITIES AT THE RGB TIP AND ON THE ZAHB, FOR TWO DIFFERENT METALLICITIES.

$M_{pr}$ <sup>a</sup>	$t_{fl}$ <sup>b</sup>	$M_{c,fl}$ <sup>c</sup>	$M_V^{0.7d}$
$Z=0.0001$			
0.8	15	0.504	—
0.9	10	0.500	0.45
1.0	6.9	0.495	0.47
1.2	3.7	0.482	0.55
1.3	2.8	0.475	0.62
1.4	2.2	0.469	0.68
1.5	1.5	0.462	0.77
1.6	1.3	0.455	0.82
1.8	1.0	0.441	0.94
1.9	0.8	0.415	1.22
2.0	0.72	0.394	1.39
2.2	0.53	0.363	—
2.3	0.46	0.335	—
2.5	0.37	0.347	—
$Z=0.0004$			
0.75	15	0.498	0.60
0.9	10	0.495	0.60
1.0	7.1	0.491	0.62
1.2	4.0	0.485	0.67
1.4	2.3	0.477	0.73
1.7	1.2	0.467	0.80
1.8	1.0	0.460	0.87
2.0	0.74	0.443	0.98

<sup>a</sup>Evolving stellar mass (solar units). <sup>b</sup> Age (Gyr) at the He ignition. <sup>c</sup> He core mass values (solar units) at the He ignition. <sup>d</sup> The absolute V magnitude at  $(V - I)_0=0.7$  mag for the ZAHB, whose RGB progenitor has the mass listed in the first column.